A role for *RAD54B* in homologous recombination in human cells

Kiyoshi Miyagawa[1,2], Takanori Tsuruga[1,3], Aiko Kinomura[1], Kiyomi Usui[1], Mari Katsura[1,3], Satoshi Tashiro[4], Hiromu Mishima[3] and Kozo Tanaka[1]

[1]Department of Molecular Pathology, Research Institute for Radiation Biology and Medicine, Hiroshima University, 1-2-3 Kasumi, Minami-ku, Hiroshima 734-8553, [3]Department of Ophthalmology and [4]Department of Biochemistry, Hiroshima University School of Medicine, 1-2-3 Kasumi, Minami-ku, Hiroshima 734-8551, Japan

[2]Corresponding author
e-mail: miyag@hiroshima-u.ac.jp

In human somatic cells, homologous recombination is a rare event. To facilitate the targeted modification of the genome for research and gene therapy applications, efforts should be directed toward understanding the molecular mechanisms of homologous recombination in human cells. Although human genes homologous to members of the *RAD52* epistasis group in yeast have been identified, no genes have been demonstrated to play a role in homologous recombination in human cells. Here, we report that *RAD54B* plays a critical role in targeted integration in human cells. Inactivation of *RAD54B* in a colon cancer cell line resulted in severe reduction of targeted integration frequency. Sensitivity to DNA-damaging agents and sister-chromatid exchange were not affected in *RAD54B*-deficient cells. Parts of these phenotypes were similar to those of *Saccharomyces cerevisiae tid1/rdh54* mutants, suggesting that *RAD54B* may be a human homolog of *TID1/RDH54*. In yeast, *TID1/RDH54* acts in the recombinational repair pathway via roles partially overlapping those of *RAD54*. Our findings provide the first genetic evidence that the mitotic recombination pathway is functionally conserved from yeast to humans.
Keywords: homologous recombination/human cells/mitosis/sister-chromatid exchange/targeted integration

Introduction

Gene targeting experiments in the chicken B-cell line DT40 and mouse embryonic stem (ES) cells have contributed to our understanding of the molecular mechanisms of homologous recombination in higher eukaryotes (Morrison and Takeda, 2000; Khanna and Jackson, 2001; Thompson and Schild, 2001). The reduced frequency of targeted integration and hypersensitivity to ionizing radiation in *RAD54* null cells have indicated that *RAD54* function is conserved from *Saccharomyces cerevisiae* to mice (Bezzubova *et al*., 1997; Essers *et al*., 1997). In contrast, *RAD51* and *RAD52* functions are not conserved throughout evolution. *RAD51* in higher eukaryotes is essential for cell viability, while yeast *RAD51* is not (Lim and Hasty, 1996; Tsuzuki *et al*., 1996). *RAD52* does not affect radiosensitivity in higher eukaryotes, while inactivation of *RAD52* in yeast results in hypersensitivity to ionizing radiation (Rijkers *et al*., 1998; Yamaguchi-Iwai *et al*., 1998). Thus, knockout experiments in DT40 and mouse ES cells have revealed that the functions of recombination genes are not always conserved from *S.cerevisiae* to mice, although their structures are well conserved throughout evolution, with the exception of *RAD52*, in which the homology is concentrated in the N-terminal part.

Despite the successful genetic manipulation of genomes of interest in DT40 and mouse ES cells, such manipulation has rarely been achieved in human cells (Yáñez and Porter, 1998; Sedivy and Dutriaux, 1999). The major obstacle to this is the low frequency of homologous recombination in humans. To improve this frequency, it is essential to understand the mechanisms of homologous recombination in human cells. It is possible that functions of recombination genes are not always conserved among higher eukaryotes. For this reason, gene targeting of these genes in human cells is indispensable.

Human *RAD54B* was isolated by screening a testis cDNA library with an expressed sequence-tagged (EST) probe homologous to *S.cerevisiae RAD54* (Hiramoto *et al*., 1999). The gene encodes a protein containing ATPase domains that are highly conserved in members of the *SWI2/SNF2* superfamily, including *RAD54*. The N-terminal half of *RAD54B* shares significant similarity with a yeast recombination gene *TID1/RDH54*, but not with *RAD54*, suggesting that *RAD54B* may be a mammalian homolog of *TID1/RDH54*. Consistent with its putative role in recombination, Rad54B forms a protein complex with Rad51, Rad54 and Brca1 (Tanaka *et al*., 2000). Rad51 is recruited to sites of DNA damage, indicating that this complex plays a role in recombinational repair of DNA damage (Tashiro *et al*., 2000).

To clarify the role of *RAD54B* in homologous recombination in humans, we generated *RAD54B*-deficient colon cancer cell lines by sequential gene targeting. The frequency of targeted integration in these cells was dramatically reduced compared with that in *RAD54B*-expressing cells. Unlike chicken and mouse mutants of other recombination genes, *RAD54B* mutants did not show hypersensitivity to DNA-damaging agents (Luo *et al*., 1999; Yamaguchi-Iwai *et al*., 1999; Deans *et al*., 2000; Takata *et al*., 2000, 2001). Sister-chromatid exchange (SCE), which was suppressed in *RAD54*-deficient DT40 and mouse ES cells (Sonoda *et al*., 1999; Dronkert *et al*., 2000), was not affected in *RAD54B* mutants. These phenotypes partially overlapped those of *S.cerevisiae tid1/rdh54* mutants (Klein, 1997; Shinohara *et al*., 1997), suggesting that *RAD54B* may be a human homolog of
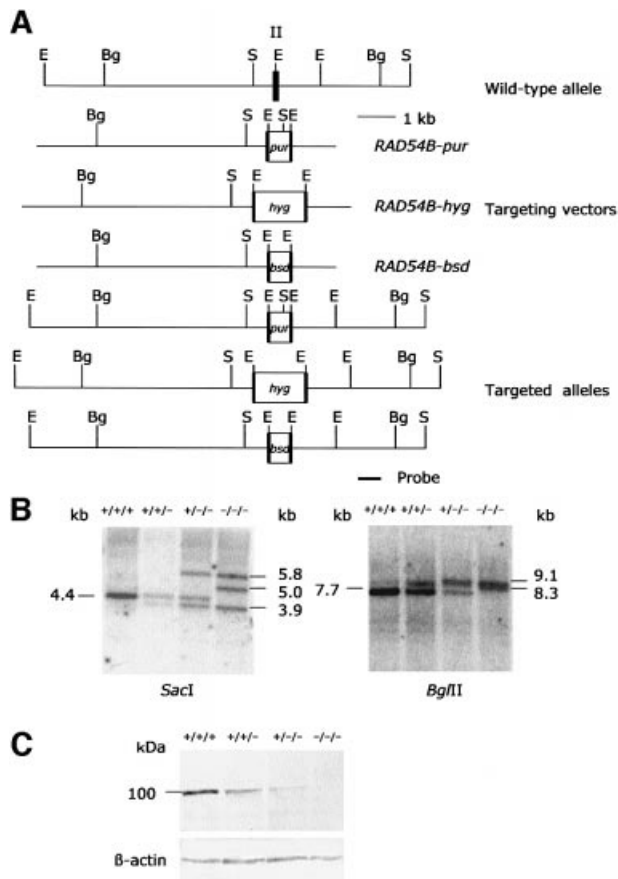
Fig. 1. Gene targeting at the human *RAD54B* locus. (**A**) Schematic representation of the *RAD54B* locus, the targeting vectors and the targeted locus. Relevant *Eco*RI (E), *Sac*I (S) and *Bgl*II (Bg) restriction sites, and the position of the probe used for Southern blot analysis are shown. Exon II is indicated by a numbered solid box. (**B**) Southern blot analysis of DNA from HCT116 cells digested with *Sac*I or *Bgl*II. Both blots were hybridized with the probe indicated in (A). (**C**) Western blot analysis of whole-cell extracts from HCT116 cells. The blot was incubated with a 1:200 dilution of anti-Rad54B antiserum.

TID1/RDH54. Thus, this system should contribute to our understanding of recombination in humans.

Results

Targeting of the RAD54B locus in HCT116 cells

Puromycin-resistant colonies generated with the *RAD54B-pur* vector were screened for targeted integration by Southern blot analysis. Insertion of the *pur* gene into the locus was expected to give 3.9 kb *Sac*I and 8.3 kb *Bgl*II fragments, in addition to 4.4 kb *Sac*I and 7.7 kb *Bgl*II wild-type fragments (Figure 1A). Two of 25 puromycin-resistant clones showed the targeted bands (Figure 1B). The *RAD54B-hyg* vector was introduced into one of these clones, *RAD54B*+/+/−p37. Hygromycin-resistant clones were screened for targeted integration. Insertion of the *hyg* gene into the locus was expected to give 5.8 kb *Sac*I and 9.1 kb *Bgl*II fragments (Figure 1A). Nine of 61 hygromycin-resistant *RAD54B*+/+/−p37 subclones showed the targeting bands without removing the *pur* gene (Figure 1B). After double knockout, the wild-type band was still present, suggesting that HCT116 cells harbor at
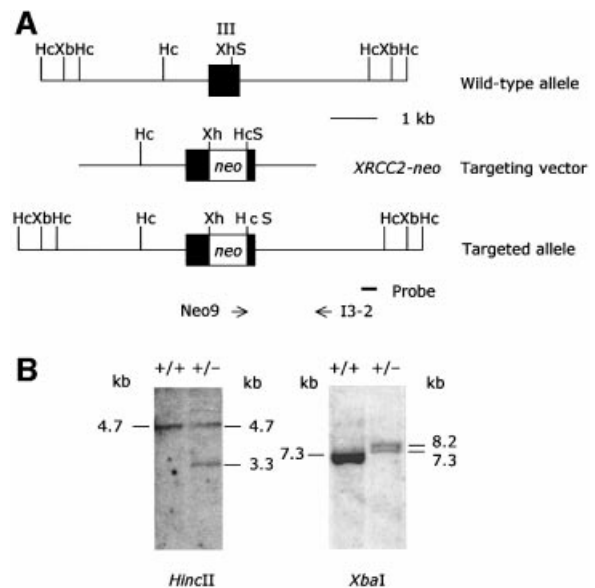
Fig. 2. Gene targeting at the human *XRCC2* locus. (**A**) Schematic representation of the *XRCC2* locus, the targeting vector and the targeted locus. Relevant *Xho*I (Xh), *Sac*I (S), *Hin*cII (Hc) and *Xba*I (Xb) restriction sites, and the position of the probe used for Southern blot analysis are shown. The positions of the primers used for PCR are indicated by arrows. Exon III is indicated by a numbered solid box. (**B**) Southern blot analysis of DNA from HCT116 cells digested with *Hin*cII or *Xba*I. Both blots were hybridized with the probe indicated in (A).

least three alleles of *RAD54B*. The *RAD54B-bsd* vector was then introduced into one of these clones, *RAD54B*+/−/−h9. Blasticidin-resistant clones were screened for targeted integration. Insertion of the *bsd* gene into the locus was expected to give 5.0 kb *Sac*I and 8.3 kb *Bgl*II fragments (Figure 1A). Two of 78 blasticidin-resistant *RAD54B*+/−/−h9 subclones showed the targeted band without removing the *pur* and *hyg* genes (Figure 1B). After triple knockout, the wild-type band disappeared. Western blot analysis revealed that the levels of Rad54B protein correlated with targeting events (Figure 1C).

Reduced frequencies of targeted integration in RAD54B-deficient cells

To examine the role of *RAD54B* in targeted integration in HCT116 cells, frequencies of targeted integration at the *XRCC2* and *RAD51L2/RAD51C* loci were analyzed. The *XRCC2-neo* vector was constructed from isogenic DNA. Targeting at the locus was expected to give 3.3 kb *Hin*cII and 8.2 kb *Xba*I fragments, in addition to 4.7 kb *Hin*cII and 7.3 kb *Xba*I wild-type fragments (Figure 2). The frequency of targeted integration in wild-type HCT116 cells was 6.4%. In single- and double-knockout cells, the frequencies were 7.5 and 8.4%, respectively. No significant difference in the frequency of targeted integration was observed between these cell lines. For measurement of the frequency in triple-knockout cells, two independent cell lines, *RAD54B*−/−/−b125 and *RAD54B*−/−/−b140, were examined. The frequencies of targeted integration at the *XRCC2* locus in these *RAD54B*-deficient cells were 0.6 and 0%, respectively, values that were reduced >10-fold compared with those for the wild-type cells (Table I). The difference in targeted integration between the wild-type and *RAD54B*-deficient cells was statistically significant. To

Table I. Frequency of targeted integration in HCT116 cells

HCT116 cells	Targeting construct			
	XRCC2-neo (%)[a]	*p* value relative to parent	*RAD51L2-neo* (%)[a]	*p* value relative to parent
RAD54B$^{+/+/+}$	6.4 (6/94)	–	0.083 (6/7197)	–
RAD54B$^{+/+/−}$p37	7.5 (7/93)	0.49	0.101 (6/5948)	0.48
RAD54B$^{+/−/−}$h9	8.4 (14/166)	0.37	0.108 (7/6509)	0.43
RAD54B$^{−/−/−}$b125	0.6 (1/173)	8.5×10^{-3}	0.010 (1/10382)	2.1×10^{-2}
RAD54B$^{−/−/−}$b140	0 (0/120)	6.6×10^{-3}	0 (0/7398)	1.4×10^{-2}
RAD54B$^{−/−/−}$b125 + *RAD54B-zeo*	15.0 (3/20)	0.95	ND	ND

[a]The frequency of targeted integration is shown as a percentage of correctly targeted clones relative to the total number of drug-resistant clones analyzed; absolute numbers are given in parentheses. The difference in frequency between *RAD54B*$^{−/−/−}$b125 and *RAD54B*$^{−/−/−}$b125 + *RAD54B-zeo* for *XRCC2-neo* was statistically significant ($p = 3.6 \times 10^{-3}$). ND, not determined. *p* values were calculated using Fisher's exact test.
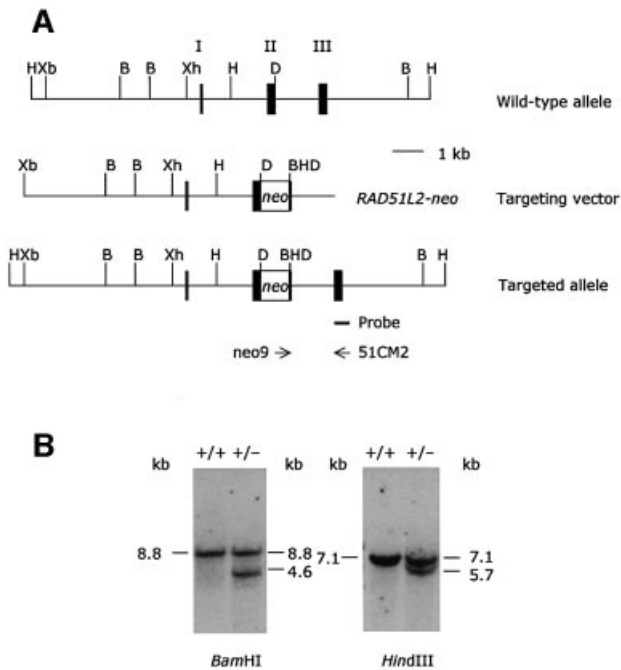

Fig. 3. Gene targeting at the human *RAD51L2/RAD51C* locus. (**A**) Schematic representation of the *RAD51L2/RAD51C* locus, the targeting vector and the targeted locus. Relevant *Xho*I (Xh), *Xba*I (Xb), *Dra*III (D), *Bam*HI (B) and *Hind*III (H) restriction sites, and the position of the probe used for Southern blot analysis are shown. The positions of the primers used for PCR are indicated by arrows. Exons I, II and III are indicated by numbered solid boxes. (**B**) Southern blot analysis of DNA from HCT116 cells digested with *Bam*HI or *Hind*III. Both blots were hybridized with the probe indicated in (A).

prove that the phenotype of *RAD54B*-deficient cells was caused by the *RAD54B* mutation, a complementation experiment was performed. *RAD54B*$^{−/−/−}$b125 cells were electroporated with a mammalian expression vector expressing the wild-type *RAD54B* cDNA and the drug-resistant marker zeocin. Cell lines that stably expressed *RAD54B* were identified from phleomycin-resistant colonies (data not shown). The frequency of targeted integration in the transformed line was 15.0%, a value that was stimulated 25-fold compared with that for *RAD54B*$^{−/−/−}$b125. Expression of the wild-type *RAD54B* cDNA corrected the targeted integration at the *XRCC2* locus to a level that was not significantly different from that of the wild-type cells ($p = 0.95$) but was significantly

different from that of *RAD54B*$^{−/−/−}$b125 cells ($p < 0.01$) (Table I).

In contrast to *XRCC2*, targeted integration at the *RAD51L2/RAD51C* locus with the *RAD51L2-neo* vector was extremely low, partly because the vector was constructed from non-isogenic DNA. Targeting at the *RAD51L2/RAD51C* locus was expected to give 4.6 kb *Bam*HI and 5.7 kb *Hind*III fragments, in addition to 8.8 kb *Bam*HI and 7.1 kb wild-type *Hind*III fragments (Figure 3). The frequency in the wild type was 0.083%. In single- and double-knockout cells, the frequencies were 0.101 and 0.108%, respectively. No significant difference in the frequency of targeted integration was observed between these cell lines. In contrast, the frequencies were 0.010 and 0% in *RAD54B*-deficient cells, values that were reduced >8-fold compared with those for the wild-type cells (Table I). The difference in targeted integration between the wild-type and *RAD54B*-deficient cells was statistically significant.

No effect of *RAD54B* on cell growth, cell survival or SCE

The growth of *RAD54B*-deficient cells was similar to that of wild-type and *RAD54B*$^{+/−/−}$ cells (Figure 4A). Sensitivity to DNA-damaging agents was monitored by the ability to form colonies after irradiation, treatment with methyl methanesulfate (MMS) or cisplatin. Cell survival assays revealed that the sensitivity of *RAD54B*-deficient cells to these agents was similar to that of wild-type and *RAD54B*$^{+/−/−}$ cells (Figure 4B–D). Compared with wild-type cells, levels of spontaneous and mitomycin C (MMC)-induced SCE were not changed in *RAD54B*-deficient cells (Figure 4E). No significant difference in karyotypes was observed among the original cell line, and the single-, double- and triple-knockout lines (data not shown).

Discussion

The present work demonstrates that *RAD54B* plays a critical role in targeted integration in human cells without affecting cell growth, cell survival to DNA-damaging agents or SCE. Since *RAD54B* shares structural similarity with *S.cerevisiae TID1/RDH54* not only in ATPase domains but also in the N-terminal region, it is probable that *RAD54B* is a human homolog of *TID1/RDH54*. The properties of the *rdh54* single mutants and the *rad54*
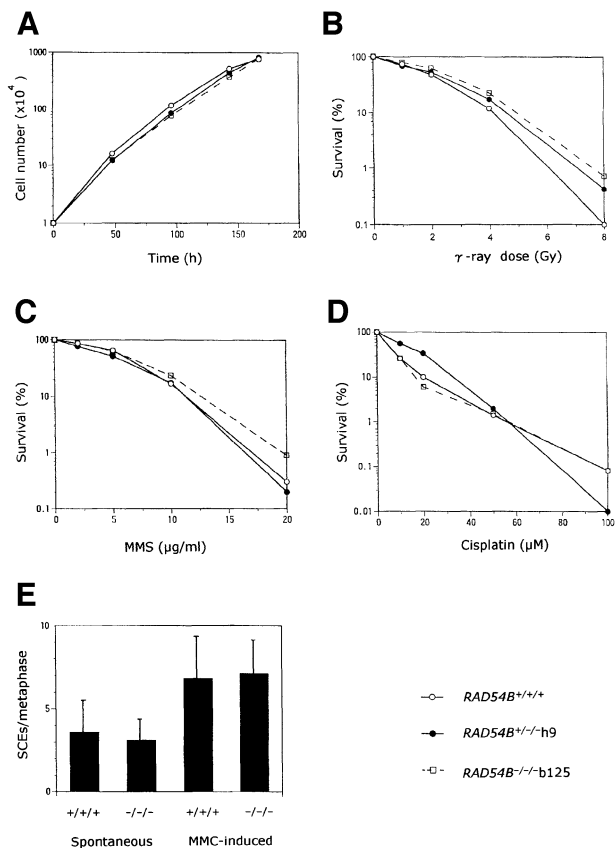
Fig. 4. Proliferative characteristics, sensitivity to DNA-damaging agents and levels of SCE of wild-type and targeted HCT116 cells. (**A**) Growth curves. (**B**) Sensitivity to ionizing radiation. (**C**) Sensitivity to MMS. (**D**) Sensitivity to cisplatin. All measurements in growth curves and cell survival were performed in triplicate. Results of representative experiments are shown here. Consistent results were obtained between different sets of experiments. (**E**) Levels of SCE. The *RAD54B*-deficient cell line used in this study was *RAD54B*$^{-/-}$b125. One hundred cells were analyzed in each preparation. The mean number of SCEs per metaphase and the standard deviation are shown.

tid1/rdh54 double mutants in mitosis and meiosis have already been characterized (Klein, 1997; Shinohara *et al.*, 1997). The yeast mutants did not show hypersensitivity to MMS. The *TID1/RDH54* gene was required for interchromosomal recombination but not for intrachromosomal gene conversion in mitosis. This phenotype was observed in the *tid1/rdh54* single mutant (Klein, 1997), whereas elsewhere it was reported that the *tid1/rdh54* single mutant did not show deficiency in mitotic recombination (Shinohara *et al.*, 1997). Interchromosomal recombination at the *HIS4* locus was reduced in the *rad54 tid1/rdh54* double mutant but not in the *tid1/rdh54* single mutant, suggesting that *TID1/RDH54* and *RAD54* act in the recombinational repair pathway with partially overlapping roles. In meiosis, the *tid/rdh54* mutant exhibited significant defects in sporulation, spore viability and recombination.

Although few comparative experiments have been performed between *RAD54B*-deficient human cells and the *tid1/rdh54* mutants, there are a couple of similarities between these mutants. First, in contrast to *RAD54* mutants in *S.cerevisiae* (Kanaar *et al.*, 1996), chickens

(Bezzubova *et al.*, 1997) and mice (Essers *et al.*, 1997), neither of these mutants showed hypersensitivity to MMS. Secondly, both mutants were defective in recombination, although the respective experiments were not comparable. The effect of *TID1/RDH54* on targeted integration, which is reduced in *RAD54* mutants in mice (Essers *et al.*, 1997), chickens (Bezzubova *et al.*, 1997), *Schizosaccharomyces pombe* (Muris *et al.*, 1997) and *S.cerevisiae* (Arbel *et al.*, 1999) as well as in *RAD54B* mutants, has not been reported. Interchromosomal recombination has been studied in *tid/rdh54* mutants. Although the relationship between targeted integration and interchromosomal recombination has not been established, they may share some similarity, since both use homologous sequences that are not present on the same chromosome. Since the roles of *RAD54B* in meiosis and the overlapping roles of *RAD54B* and *RAD54* in humans remain to be demonstrated, we are not able to conclude that *RAD54B* is the functional homolog of the yeast *TID1/RDH54* gene. However, our findings indicate that some, if not all, roles in the recombinational repair pathway in mitosis might be conserved between *RAD54B* and *TID1/RDH54*.

In the mitotic cell cycle of yeast, *RAD54* is essential for repair by the sister chromatid, whereas *TID1/RDH54* is not required for this pathway (Arbel *et al.*, 1999). The role for *RAD54* in sister-chromatid-based repair may be conserved from yeast to higher eukaryotes. *RAD54*-deficient DT40 cells have been shown to be extremely sensitive to ionizing radiation in G$_2$ as well as G$_1$, while wild-type DT40 cells were resistant to irradiation in G$_2$ (Takata *et al.*, 1998). The sister chromatids serve as the main template for recombination in G$_2$. Therefore, hypersensitivity to irradiation of the *RAD54* mutant in G$_2$ implies that *RAD54* is required for DNA repair mediated by sister chromatids. Consistent with this idea, DNA damage-induced SCE was reduced in *RAD54*-deficient DT40 and mouse ES cells (Sonoda *et al.*, 1999; Dronkert *et al.*, 2000). These phenotypes of *RAD54* mutants were not observed in either human *RAD54B*-deficient cells or yeast *tid1/rdh54* mutants, supporting the idea that *RAD54* acts in homologous recombination in a pathway distinct from that of *RAD54B*. However, given that both mutations in mammals show synergic defects in recombination, *RAD54B* and *RAD54* may act in the recombinational pathway with partially overlapping roles.

Rad54B forms a protein complex with Rad51, Rad54 and Brca1 (Tanaka *et al.*, 2000). In *RAD54*-deficient ES cells, Rad51 focus formation has been shown to be blocked (Tan *et al.*, 1999). In analogy with *RAD54*, inactivation of *RAD54B* may result in the reduction of Rad51 focus formation. Another possible scenario for the effect of Rad54B on the protein complex is that Rad54B may affect the colocalization of Rad51 and other proteins that play a role in recombination. In the meiotic cell cycle of yeast *tid1/rdh54* mutants, the colocalization of Rad51 and Dmc1 has been shown to be reduced, although Rad51 formed foci (Shinohara *et al.*, 2000). *DMC1* is only expressed in meiosis (Bishop *et al.*, 1992). There may be other proteins that interact with Rad51 and Rad54B in the mitotic recombination pathway.

RAD54B plays a unique role in homologous recombination because it does not affect the sensitivity to DNA-damaging agents. With the exception of *RAD52*, other

recombination genes, including *RAD51*, *RAD54*, *MRE11* and *RAD51* paralogs, do affect the sensitivity to such agents. To improve targeted integration in the human genome, it will be important to modify the functions of genes that play a central role in targeted integration without affecting other cellular properties. *RAD54B* is an excellent candidate for such modification. Targeted integration events were hardly detectable in *RAD54B*-deficient cells in the present study. In *RAD52*-deficient ES cells, no such drastic reduction of targeted integration has been reported (Rijkers *et al.*, 1998). Thus, this system provides new insight into genetic manipulation of the human genome.

Materials and methods

Construction of RAD54B targeting vectors
Promoterless targeting vectors were designed to insert drug resistance genes in exon 2 in-frame. The right homology arm was isolated as a 1.2 kb *Eco*RI fragment from the EMBL3 SP6/T7 human genomic library (Clontech) and inserted into pBluescript SK. A 3′ 130 bp fragment with the *Eco*RI site was deleted with a combination of exonuclease III and S1 nuclease digestion. The left homology arm was isolated as a 6.4 kb *Eco*RI fragment from the same library and inserted into the unique *Eco*RI site of the vector containing the right arm. The 5′ *Eco*RI site was removed by treatment with exonuclease III and S1 nuclease. A puromycin resistance cassette was amplified from pKO SelectPuro (Lexicon Genetics) with puro-1 (5′-GCGAATTCCATGACCGAGTACAAG-3′) and BGHpA-2 (5′-GCGAATTCGCCTGCTATTGTCTTCC-3′) and inserted into the *Eco*RI site of the targeting vector. A hygromycin resistance cassette was generated from pcDNA3.1/Hygro (Invitrogen) by PCR. Since the coding sequence for this cassette contains an *Eco*RI site, PCR was performed with mismatch primers converting the *Eco*RI to a *Hin*dIII site without loss of hygromycin resistance. Upstream of the *Eco*RI site was amplified with hyg1 (5′-GCCGAATTCGATGAAAAAGCCTGA-3′) and hyg2 (5′-CG-GAATTCAAGCTTCCAATGTCAAGC-3′) and inserted into the *Eco*RI site of the vector containing both arms. Downstream of the *Eco*RI site was amplified with hyg3 (5′-ATAAGCTTCAGCGAGAGCCTG-3′) and hyg4 (5′-CGAAGCTTTCATTAGGCACC-3′) and inserted into the *Hin*dIII site converted from the *Eco*RI site by hyg2. A blasticidin resistance cassette was amplified from pCMV/Bsd (Invitrogen) with BSD-1 (5′-GCGAATTCCATGGCCAAGCCTTTG-3′) and BSD-2 (5′-CCGGGA-ATTCAGACATG-3′) and inserted into the *Eco*RI of the targeting vector. The sequences of all PCR products were confirmed.

Generation of RAD54B-deficient cells
HCT116 cells derived from human colon carcinoma (ATCC CCL-247) were cultured in McCoy's 5A medium with 10% fetal calf serum. Targeting vectors linearized with *Kpn*I were introduced into 2×10^7 cells using a Bio-Rad Gene Pulsar at 1200 V and 50 µF. For selection of targeted cells, hygromycin, puromycin and blasticidin were added at 200, 1.25 and 20 µg/ml, respectively. After 14 days, colonies were isolated and expanded. Genomic DNA from individual colonies was digested with *Sac*I or *Bgl*II and subjected to Southern blot analysis. The blots were hybridized with an external probe 3′ of the targeting constructs. Western blot analysis was performed as described previously (Tanaka *et al.*, 2000).

Expression of the RAD54B cDNA
The human *RAD54B* cDNA (DDBJ/EMBL/GenBank accession No. AF112481) was cloned into the pcDNA3.1/Zeo(+) mammalian expression vector (Invitrogen) and checked by sequencing. The vector was transfected into *RAD54B*-deficient cells by electroporation and selected with 240 µg/ml phleomycin (Sigma).

Construction of the XRCC2 targeting vector
A promoterless targeting vector was designed to insert a neomycin resistance cassette at the *Xho*I site in exon 3 in-frame. The 1.6 kb right homology arm was amplified from isogenic DNA of HCT116 cells with E3-1 (5′-GTAGTCACCCATCTCTCT-3′) and I3-1 (5′-TCTTTGCCTG-TGCCTATG-3′) and inserted into pCR2.1 (Invitrogen) by the TA cloning method. A neomycin resistance cassette was amplified from pMC1neo-polyA (Stratagene) with S-X-neo (5′-ATGAGCTCGAGCATGGGA-TCGGCCATT-3′) and neo8-S (5′-TGAGCTCAAGCTTGGCTGCAG-

GT-3′) and replaced with a 244 bp exonic fragment flanked with *Sac*I in the right arm vector. The 2.7 kb left homology arm was amplified from the isogenic DNA with I2-1 (5′-CTCCTGGGTTCAACTGAT-3′) and E3-2 (5′-TCTTCTGATGAGCTCGAG-3′) and inserted into pCR2.1. A 56 bp *Xho*I fragment was replaced with a 2.3 kb *Xho*I fragment released from the right arm vector containing both the neomycin resistance cassette and the right arm.

Measurement of targeted integration frequencies at the XRCC2 locus
The *XRCC2-neo* vector was introduced into 2×10^7 wild-type or *RAD54B* mutant HCT116 cells by electroporation. After 24 h, G418 was added to a final concentration of 400 µg/ml. After selection, DNA was extracted from individual colonies. Targeted integration events were screened by PCR with neo9 (5′-ATCGGCCTTCTTGACGAGT-3′) and I3-2 (5′-TTGGCGTCTTCGTCATGA-3′). Southern blot analysis was also used to confirm targeted integration. Genomic DNA was digested with *Hin*cII or *Xba*I and the blots were hybridized with an external probe.

Construction of the RAD51L2/RAD51C targeting vector
A promoterless targeting vector was designed to insert a neomycin resistance cassette at the *Dra*III site in exon 2 in-frame. A 4.4 kb *Xho*I fragment containing exons 1 and 2 was isolated from the EMBL3 SP6/T7 human genomic library and inserted into pUC19. A neomycin resistance cassette was amplified from pMC1neo-polyA (Stratagene) with neodras (5′-CGCACCCAGGTGCCAATATGGGATCGGCCA-3′) and neodraas (5′-GGCACCTGGTGAAGCTTGGCTGCAGGTC-3′) and inserted at the *Dra*III site in exon 2. A 5.1 kb *Xba*I–*Xho*I fragment containing the promoter region upstream of exon 1 was isolated from the same library and inserted into pBluescript SK. A 5.3 kb *Xho*I fragment with the neomycin resistance cassette released from the pUC19 vector was inserted into the *Xho*I site of the pBluescript vector with the upstream region.

Measurement of targeted integration frequencies at the RAD51L2/RAD51C locus
The *RAD51L2-neo* targeting vector was introduced into $1.5–3.7 \times 10^8$ wild-type or *RAD54B* mutant HCT116 cells by electroporation. After 24 h, G418 was added to a final concentration of 400 µg/ml. After selection, DNA was extracted from pools of 20–100 colonies. Targeted integration events were screened by PCR with neo9 and 51CM2 (5′-TGCACATCTACTGCCAAC-3′). To test for PCR conditions, a control vector that included the annealing site for 51CM2 was constructed and introduced into HCT116 cells. PCR conditions were optimized to detect a single targeted integration event in a pool of 100 negative G418-resistant cells. To confirm the targeting event by Southern blot analysis, single positive clones were obtained from positive pools of G418-resistant colonies by limiting dilution. Their genomic DNA was subjected to Southern blot analysis; the blots were hybridized with a probe outside the targeting vector.

Analysis of cell growth
HCT116 cells were plated at a density of 10^4 cells per 60 mm dish and cultured. On the days indicated, cells were counted. All measurements were performed in triplicate.

Cell survival assay
HCT116 cells were plated at a density of 10^3 cells per 60 mm dish and irradiated with a ^{60}Co source or treated with MMS (Sigma). To measure sensitivity to cisplatin (Nihon-Kayaku), cells were incubated in the presence of cisplatin for 1 h and washed twice. The cells were grown for 7 days and, after fixing and staining, colonies were counted. All measurements were performed in triplicate.

Analysis of SCEs
Cells were cultured in 16 µM 5-bromodeoxyuridine (BUdR) for 36 h and pulsed with 0.1 µg/ml colcemid for the last 1 h. To examine MMC-induced SCEs, cells were incubated in the presence of 0.8 µg/ml MMC for 8 h. Harvested cells were treated with 75 mM KCl:1% sodium citrate (4:1) for 20 min and fixed with methanol:acetic acid (3:1). Cells were fixed on slides and incubated with 12.8 µg/ml Hoechst 33258 for 20 min. The slides were irradiated with ultraviolet radiation ($\lambda = 352$ nm) for 1 h at 60°C and stained with 4% Giemsa solution. The cell lines were coded to prevent bias in the analysis.

Acknowledgements

References

Arbel,A., Zenvirth,D. and Simchen,G. (1999) Sister chromatid-based DNA repair is mediated by *RAD54*, not by *DMC1* or *TID1*. *EMBO J.*, **18**, 2648–2658.

Bezzubova,O., Silbergleit,A., Yamaguchi-Iwai,Y., Takeda,S. and Buerstedde,J.-M. (1997) Reduced X-ray resistance and homologous recombination frequencies in a *RAD54*−/− mutant of the chicken DT40 cell line. *Cell*, **89**, 185–193.

Bishop,D.K., Park,D., Xu,L. and Kleckner,N. (1992) *DMC1*: a meiosis-specific yeast homolog of *E. coli* recA required for recombination, synaptonemal complex formation, and cell cycle progression. *Cell*, **69**, 439–456.

Deans,B., Griffin,C.S., Maconochie,M. and Thacker,J. (2000) *Xrcc2* is required for genetic stability, embryonic neurogenesis and viability in mice. *EMBO J.*, **19**, 6675–6685.

Dronkert,M.L.G., Beverloo,H.B., Johnson,R.D., Hoeijmakers,J.H.J., Jasin,M. and Kanaar,R. (2000) Mouse *RAD54* affects DNA double-strand break repair and sister chromatid exchange. *Mol. Cell. Biol.*, **20**, 3147–3156.

Essers,J., Hendriks,R.W., Swagemakers,S.M.A., Troelstra,C., de Wit,J., Bootsma,D., Hoeijmakers,J.H.J. and Kanaar,R. (1997) Disruption of mouse *RAD54* reduces ionizing radiation resistance and homologous recombination. *Cell*, **89**, 195–204.

Hiramoto,T. *et al.* (1999) Mutations of a novel human *RAD54* homologue, *RAD54B*, in primary cancer. *Oncogene*, **18**, 3422–3426.

Kanaar,R. *et al.* (1996) Human and mouse homologs of the *Saccharomyces cerevisiae RAD54* DNA repair gene: evidence for functional conservation. *Curr. Biol.*, **6**, 828–838.

Khanna,K.K. and Jackson,S.P. (2001) DNA double-strand breaks: signaling, repair and the cancer connection. *Nature Genet.*, **27**, 247–254.

Klein,H.L. (1997) RDH54, a *RAD54* homologue in *Saccharomyces cerevisiae*, is required for mitotic diploid-specific recombination and repair and for meiosis. *Genetics*, **147**, 1533–1543.

Lim,D.-S. and Hasty,P. (1996) A mutation in mouse *rad51* results in an early embryonic lethal that is suppressed by a mutation in *p53*. *Mol. Cell. Biol.*, **16**, 7133–7143.

Luo,G., Yao,M.S., Bender,C.F., Mills,M., Bladl,A.R., Bradley,A. and Petrini,J.H.J. (1999) Disruption of *mRad50* causes embryonic stem cell lethality, abnormal embryonic development, and sensitivity to ionizing radiation. *Proc. Natl Acad. Sci. USA*, **96**, 7376–7381.

Morrison,C. and Takeda,S. (2000) Genetic analysis of homologous DNA recombination in vertebrate somatic cells. *Int. J. Biochem. Cell Biol.*, **32**, 817–831.

Muris,D.F.R., Vreeken,K., Schmidt,H., Ostermann,K., Clever,B., Lohman,P.H.M. and Pastink,A. (1997) Homologous recombination in the fission yeast *Schizosaccharomyces pombe*: different requirements for the *rhp51*+, *rhp54*+ and *rad22*+ genes. *Curr. Genet.*, **31**, 248–254.

Rijkers,T., van den Ouweland,J., Morolli,B., Rolink,A.G., Baarends, W.M., van Sloun,P.P.H., Lohman,P.H.M. and Pastink,A. (1998) Targeted inactivation of mouse *RAD52* reduces homologous recombination but not resistance to ionizing radiation. *Mol. Cell. Biol.*, **18**, 6423–6429.

Sedivy,J.M. and Dutriaux,A. (1999) Gene targeting and somatic cell genetics: a rebirth or a coming of age? *Trends Genet.*, **15**, 88–90.

Shinohara,M., Shita-Yamaguchi,E., Buerstedde,J.-M., Shinagawa,H., Ogawa,H. and Shinohara,A. (1997) Characterization of the roles of the *Saccharomyces cerevisiae RAD54* gene and a homologue of *RAD54*, *RDH54/TID1*, in mitosis and meiosis. *Genetics*, **147**, 1545–1556.

Shinohara,M., Gasior,S.L., Bishop,D. and Shinohara,A. (2000) Tid1/ Rdh54 promotes colocalization of Rad51 and Dmc1 during meiotic recombination. *Proc. Natl Acad. Sci. USA*, **97**, 10814–10819.

Sonoda,E., Sasaki,M.S., Morrison,C., Yamaguchi-Iwai,Y., Takata,M. and Takeda,S. (1999) Sister chromatid exchanges are mediated by homologous recombination in vertebrate cells. *Mol. Cell. Biol.*, **19**, 5166–5169.

Takata,M. *et al.* (1998) Homologous recombination and non-homologous end-joining pathways of DNA double-strand break repair have overlapping roles in the maintenance of chromosomal integrity in vertebrate cells. *EMBO J.*, **17**, 5497–5508.

Takata,M. *et al.* (2000) The Rad51 paralog Rad51B promotes homologous recombinational repair. *Mol. Cell. Biol.*, **20**, 6476–6482.

Takata,M., Sasaki,M.S., Tachiiri,S., Fukushima,T., Sonoda,E., Shild,D., Thompson,L.H. and Takeda,S. (2001) Chromosome instability and defective recombinational repair in knockout mutants of the five Rad51 paralogs. *Mol. Cell. Biol.*, **21**, 2858–2866.

Tan,T.L.R., Essers,J., Citterio,E., Swagemakers,S.M.A., de Wit,J., Benson,F.E., Hoeijmakers,J.H.J. and Kanaar,R. (1999) Mouse Rad54 affects DNA conformation and DNA-damage-induced Rad51 foci formation. *Curr. Biol.*, **9**, 325–328.

Tanaka,K., Hiramoto,T., Fukuda,T. and Miyagawa,K. (2000) A novel human Rad54 homologue, Rad54B, associates with Rad51. *J. Biol. Chem.*, **275**, 26316–26321.

Tashiro,S., Walter,J., Shinohara,A., Kamada,N. and Cremer,T. (2000) Rad51 accumulation at sites of DNA damage and in postreplicative chromatin. *J. Cell Biol.*, **150**, 283–291.

Thompson,L.H. and Schild,D. (2001) Homologous recombinational repair of DNA ensures mammalian chromosome stability. *Mutat. Res.*, **477**, 131–153.

Tsuzuki,T., Fujii,Y., Sakumi,K., Tominaga,Y., Nakao,K., Sekiguchi,M., Matsushiro,A., Yoshimura,Y. and Morita,T. (1996) Targeted disruption of the *Rad51* gene leads to lethality in embryonic mice. *Proc. Natl Acad. Sci. USA*, **93**, 6236–6240.

Yamaguchi-Iwai,Y., Sonoda,E., Buerstedde,J.-M., Bezzubova,O., Morrison,C., Takata,M., Shinohara,A. and Takeda,S. (1998) Homologous recombination, but not DNA repair, is reduced in vertebrate cells deficient in RAD52. *Mol. Cell. Biol.*, **18**, 6430–6435.

Yamaguchi-Iwai,Y. *et al.* (1999) Mre11 is essential for the maintenance of chromosomal DNA in vertebrate cells. *EMBO J.*, **18**, 6619–6629.

Yáñez,R.J. and Porter,A.C.G. (1998) Therapeutic gene targeting. *Gene Ther.*, **5**, 149–159.